POLISH
JOURNAL *of* RADIOLOGY

Original paper

# A radiomic signature based on magnetic resonance imaging to determine adrenal Cushing's syndrome

Ferhat Can Piskin[A,B,C,D,E,F,G], Gamze Akkus[A,B,C,D,E,F,G], Sevinc Puren Yucel[A,C,D,E], Bisar Akbas[B,E], Fulya Odabası[A,B]

Cukurova University Medical Faculty, Adana, Turkey

## Abstract

**Purpose**: The aim of this study was to develop radiomics signature-based magnetic resonance imaging (MRI) to determine adrenal Cushing's syndrome (ACS) in adrenal incidentalomas (AI).

**Material and methods**: A total of 50 patients with AI were included in this study. The patients were grouped as non-functional adrenal incidentaloma (NFAI) and ACS. The lesions were segmented on unenhanced T1-weighted (T1W) in-phase (IP) and opposed-phase (OP) as well as on T2-weighted (T2-W) 3-Tesla MRIs. The LASSO regression model was used for the selection of potential predictors from 111 texture features for each sequence. The radiomics scores were compared between the groups.

**Results**: The median radiomics score in T1W-Op for the NFAI and ACS were –1.17 and –0.17, respectively ($p < 0.001$). Patients with ACS had significantly higher radiomics scores than NFAI patients in all phases ($p < 0.001$ for all). The AUCs for radiomics scores in T1W-Op, T1W-Ip, and T2W were 0.862 (95% CI: 0.742-0.983), 0.892 (95% CI: 0.774-0.999), and 0.994 (95% CI: 0.982-0.999), respectively.

**Conclusion**: The developed MRI-based radiomic scores can yield high AUCs for prediction of ACS.

**Key words**: non-functioning adrenal incidentalomas, adrenal Cushing's syndrome, magnetic resonance imaging, machine learning.

## Introductions

Adrenal incidentalomas (AI) are adrenal masses detected on imaging for diseases other than adrenal diseases. AI is detected in 5% of patients undergoing radiological imaging. The incidence of AI is increasing with the further use of radiological imaging in the clinic [1]. The almost guidelines suggest that AIs should be investigated for malign or benign nodules because the most common cause of adrenal masses is metastasis of malignant tumours [2]. This distinction can be made highly accurately with clinical history and conventional radiological imaging. The second most common cause of AIs is adrenal adenomas. If AI exhibits lower density on unenhanced computed tomography (CT) than 10 Hounsfield units (HU), it can be diagnosed with confidence (sensitivity of 71% and specificity of 98%) and is referred to as a fat-rich adenoma. In addition, the adrenal adenoma can be distinguished from malign adrenal masses by showing wash-out on enhanced CT and chemical shift in dual-echo sequences on magnetic resonance imaging (MRI) [3].

The guidelines recommend that adrenal adenoma should be analysed in terms of functionality on the second step duration at diagnosis [2,4]. Adrenal adenomas are divided into subgroups as non-functional AI (NFAI), autonomous mild cortisol-secreting AI (ACSAI), aldosterone-producing adenoma (APA), pheochromocytoma, and adrenal Cushing's syndrome (ACS) [5]. With conventional radiological imaging, adrenal adenomas are not tested for functionality and cannot be distinguished into subgroups. For this distinction, clinical evaluation and detailed endocrine tests such as 1 mg dexamethasone and 24-hour

**Correspondence address:**

Ferhat Can Piskin, Cukurova University Medical Faculty, Adana, Turkey, e-mail: ferhatcpiskin@gmail.com

urine cortisol are required. Due to these laborious tests, the majority of patients refuse further examinations, and the AIs remain indeterminate [2].

Radiomics is the texture analysis of conventional radiological images with specific software and obtaining properties that cannot be detected by the human eye. Virtual tissue analysis can be performed on tumours by using radiomics. Recent studies indicate that distinguishing between malign or benign adrenal nodules is feasible with texture analysis. It has also been established in a few studies that APAs can be detected with high accuracy using radiomics analysis [5-7]. As far as we know, there are no radiomics studies investigating ACS in AIs.

Therefore, the aim of this study was to develop a radiomics signature-based MRI to determine ACS in AIs.

## Material and methods

### Patient population

All consecutive patients diagnosed with AI on MRI between 2015 and 2021 were included in the study. The inclusion criteria were determined as NFAI or AI compatible with ACS by the endocrinological evaluation, and solid and unilateral features of the adrenal mass. The adrenal lesion was not suitable for segmentation due to respiratory artifacts on MRI, known ACSAI, pheochromocytoma, or APA as exclusion criteria.

The Institutional Clinical Research Ethical Committee approved this single-centre retrospective study. Informed consent was obtained from all patients before all diagnostic procedures according to the 1964 Helsinki Declaration principles.

### Endocrinological evaluation

The diagnosis of ACS was made on the basis of biochemical tests including serum cortisol and plasma adrenocorticotrophic hormone (ACTH) levels, urinary free cortisol, and overnight low-dose dexamethasone suppression testing. ACS was diagnosed in the presence of classical clinical signs and symptoms. All patients underwent baseline cortisol, ACTH measurement, and 1 mg overnight dexamethasone suppression test (DST). Patients with NFAI whose cortisol levels were suppressed ($\leq 1.8$ µg/dl) following the midnight 1 mg DST, with normal 24-hour metanephrine-normetanephrine levels in urine, and plasma aldosterone (ng/dl)/renin (ng/ml/h) ratio < 20 were considered "non-functional". Interpretation of the 1 mg overnight DST results is based on the guidelines [2].

### Magnetic resonance imaging

All MRI scanning was acquired using a 3.0-T MRI (Ingenia, Philips Medical Systems, Netherlands). MRI protocol included T1-weighted (T1W) chemical shift (CS), in-phase (Ip) and opposed-phase (Op) imaging, and turbo spin-echo T2-weighted (T2W) on the axial plane. The specific parameters of MRI were as follows: T1-W chemical shift spoiled gradient echo sequence on the axial plane (TR/ TE = 1500/1.37 and 2.27 ms; slice thickness = 3 mm; interslice gap = 0.6 mm; matrix = 320 × 182; field of view = 400 × 400), half Fourier single-shot turbo spin-echo T2W sequence on the axial plane (TR/TE = 2000/90 ms; slice thickness = 3 mm; interslice gap = 0.6 mm; matrix = 256 × 179; field of view = 400 × 400).

### Segmentation and texture analysis

DICOM data was transferred to dedicated software (Olea sphere v.3 SP2, Olea Medical, France) for segmentation and texture analysis of adrenal lesions. The boundaries of the adrenal lesion were manually drawn slice-by-slice on T1W-Ip and T1W-Op imaging and T2-weighted (T2W) images. A volume of interest (VOI) covering the entire lesion was created. The images were normalized using the Z score to eliminate the possible effects of protocol and scan parameters. A total of 111 grey level properties (first and second-order) of the generated VOI were extracted.

### Radiomics feature selection

The least absolute shrinkage and selection operator (LASSO) method, proposed by Tibshirani (1996), is a widely used algorithm for the reduction of high-dimensional data and variable selection, especially in radiomics studies in recent years. Basically, LASSO minimizes the regression coefficients of redundant features to determine the best subset of radiomics features.

In this study, a total of 111 features were extracted for each patient based on MRI, and the radiomics feature selection process was carried out using the LASSO method. The LASSO method was combined with logistic regression to select the features most associated with Cushing's syndrome from 111 candidate radiomics features. The "glmnet" package was used in R software for LASSO logistic regression. First, the LASSO tuning parameter ($\lambda$), which gives the maximum area under the curve (AUC) and the minimum cross-validation error, is determined. Using the minimum criteria in 5-fold cross-validation with 100 replications, the value of the optimal tuning parameter that the model best fitted to the data was determined as $\lambda = 0.09749558$ in T1W-Op, $\lambda = 0.07921766$ in T1W-Ip, and $\lambda = 0.02147446$ in T2W. Non-zero radiomics features were selected with the tuning parameter determined in each phase, and the radiomics score was calculated for each patient by a linear combination of the selected radiomics features with their respective coefficients.

### Statistical analysis

Categorical variables were expressed as numbers and percentages, whereas continuous variables were summa-

rized as mean and standard deviation and as median and minimum-maximum where appropriate. The chi-square test was used to compare sexes between the groups. The normality of distribution for continuous variables (age, radiomics scores) was confirmed with the Shapiro-Wilk test. For comparison of continuous variables between 2 groups, Student's *t*-test or the Mann-Whitney *U* test was used depending on whether the statistical hypotheses were fulfilled. The distribution of radiomics scores in the study groups is shown with the violin (violin) graph. The „ggplot2" package was used for violin plots. The performance of radiomics scores was evaluated by receiver operating characteristic (ROC) curve analysis and performance measures (area under the curve-AUC, sensitivity, specificity, accuracy) were obtained. The best cut-off point was determined according to the IU method [8].

The resulting AUCs were compared using DeLong's test. The statistical level of significance for all tests was 0.05. The statistical analysis was performed using R software version 3.3.2 and IBM SPSS Statistics version 20.0.

## Results

A total of 50 patients with AI were included in this study. There were 16 patients in the ACS group, including 15 (93.8%) males and one (6.2%) female, with mean age 59.7 ± 10.7 years (median, 61.0 years). There were 34 patients in the NFAI group, including 19 (55.9%) males and 15 (44.1%) females, with mean age 47.8 ± 14.1 years (median, 58.0 years). There were no significant differences in age ($p = 0.325$) between the 2 groups but a significant difference in sex ($p = 0.019$).

According to 5-fold cross-validation, 111 extracted features were reduced to 5, 5, and 12 potential predictors for T1W-Op, T1W-Ip, and T2W radiomics score construction, respectively, using the LASSO logistic regression model. Details of the selected features are shown in Table 1, and the distribution of the radiomics scores is given in Figure 1.

The median radiomics scores in T1W-Op for the NFAI and ACS were –1.17 and –0.17, respectively ($p <0.001$).

**Table 1.** Selected features for the T1-weighted opposed-phase (T1W-Op), T1-weighted in-phase (T1W-Ip), and T2-weighted (T2W) phase

| Phase of magnetic resonance imaging | | | | | |
|---|---|---|---|---|---|
| T1W-Op (*n* = 50) | | T1W-Ip (*n* = 50) | | T2W (*n* = 50) | |
| Feature | Coefficient | Feature | Coefficient | Feature | Coefficient |
| Intercept | 0.3755253 | Intercept | −1.255187 | Intercept | −2.560467 |
| Original Shape Voxel Volume | 0.00003600333 | Original Shape Mesh Volume | 0.00003152016 | Original Shape Maximum 2D Diameter Column | 0.004528224 |
| Original Shape Surface Area to Volume Ratio | −1.919865 | Original Shape Minor Axis Length | 0.006888999 | Original Shape Maximum 2D Diameter Row | 0.07499843 |
| Original Shape Minor Axis Length | 0.01097283 | Original First Order Standard Deviation | −6.718571 | Original First Order Standard Deviation | −9.306228 |
| Original First Order Standard Deviation | 3.595912 | Original Grey Level Size Zone Matrix Large Area High Grey Level Emphasis | 0.000003923087 | Original First Order Skewness | −2.226719 |
| Original Gray Level Size Zone Matrix Large Area Emphasis | 0.02029405 | Original Grey Level Dependence Matrix Large Dependence Emphasis | 0.2650397 | Original Grey Level Co-occurrence Matrix Cluster Prominence | −0.00000089917 |
| | | | | Original Grey Level Co-occurrence Matrix Joint Energy | 758.0025 |
| | | | | Original Grey Level Run Length Matrix Run Variance | 37.35687 |
| | | | | Original Grey Level Run Length Matrix Long Run Low Grey Level Emphasis | 4.236102 |
| | | | | Original Grey Level Size Zone Matrix Small Area High Grey Level Emphasis | −0.003970735 |
| | | | | Original Neighbouring Gray Tone Difference Matrix Coarseness | 36.6343 |
| | | | | Original Neighbouring Grey Tone Difference Matrix Busyness | 2.882380 |
| | | | | Original Grey Level Dependence Matrix Large Dependence Low Grey Level Emphasis | 1.076042 |

Features were selected via LASSO modelling. A set of 5, 5, and 12 features were selected in the T1W-Op, T1W-Ip, and T2W phases, respectively.
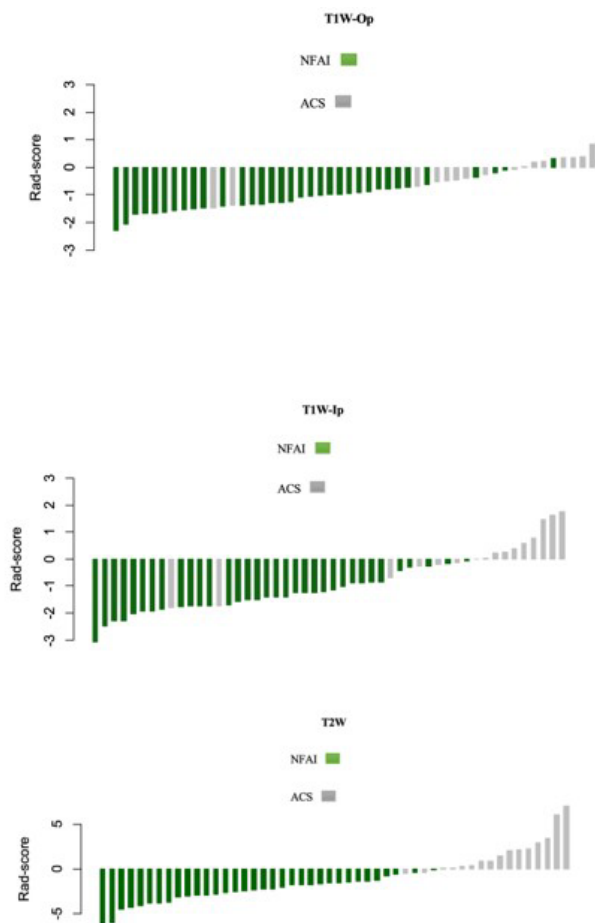
**Figure 1.** Distribution of radiomics scores, Waterfall plot. Grey bars show radiomics scores for patients with adrenal cushing syndrome (ACS); green bars show radiomics scores for patients with non-functional adrenal incidentaloma (NFAI). T1W –T1-weighted, Op –opposed-phase, Ip – in-phase, T2W – T2-weighted

**Table 2.** Radiomics score distributions between the groups

| Radiomics score | Groups | | p-value |
| | NFAI (n = 34) | ACS (n = 16) | |
|---|---|---|---|
| T1W-Op | −1.13 ± 0.55 −1.17 (−2.29-0.33) | −0.21 ± 0.64 −0.17 (−1.48-0.85) | < 0.001 |
| T1W-Ip | −1.39 ± 0.68 −1.41 (−3.08 to −0.07) | 0.15 ± 1.02 0.13 (−1.79-1.78) | < 0.001 |
| T2W | −2.53 ± 1.45 −2.31 (−6.33 to −0.12) | 1.81 ± 2.19 1.18 (−0.46-7.04) | < 0.001 |

NFAI – non-functional adrenal incidentaloma, ACS – adrenal Cushing's syndrome, T1W – T1-weighted, Op – opposed-phase, Ip – in-phase, T2W – T2-weighted

**Table 3.** Predictive performance of the radiomics scores

| | Cut-off | Sensitivity | Specificity | Accuracy | AUC (95% CI) | p-value |
|---|---|---|---|---|---|---|
| Radiomics score (T1W-Op) | −0.69 | 0.88 | 0.85 | 0.86 | 0.862 (0.742-0.983) | < 0.001 |
| Radiomics score (T1W-Ip) | −0.78 | 0.88 | 0.85 | 0.86 | 0.892 (0.774-0.999) | < 0.001 |
| Radiomics score (T2W) | −0.44 | 0.94 | 0.97 | 0.94 | 0.994 (0.982-0.999) | < 0.001 |

T1W – T1-weighted, Op – opposed-phase, Ip – in-phase, T2W – T2-weighted

Patients with ACS had significantly higher radiomics scores than NFAI patients in all phases ($p < 0.001$ for all) (Table 2).

Table 3, Figure 2, and Figure 3 show the diagnostic performance of the radiomics score in discrimination between NFAI and ACS. The AUCs for radiomics scores in T1W-Op, T1W-Ip, and T2W were 0.862 (95% CI: 0.742-0.983), 0.892 (95% CI: 0.774-0.999), and 0.994 (95% CI: 0.982-0.999), respectively. The performance of the radiomics score in T2W was significantly higher than in T1W-Op ($p = 0.028$). In addition, the radiomics score in T1W-Ip showed similar discrimination performance as the radiomics scores in T1W-Op and T2W ($p = 0.195$, $p = 0.086$, respectively). Although the AUC values of T1W-Ip and T2W were similar, the sensitivity and specificity were higher in T2W (Figure 3).

## Discussion

ACS is associated with poor quality of life, morbidity, and 5-fold higher mortality. The patients may present with central obesity, thinned skin with wide purple striae, fatigue, proximal muscle weakness, hypertension, glucose intolerance, acne, and hirsutism [9]. Because manifestations of ACS are variable, the diagnosis may be challenging when signs and symptoms are subtle. And symptoms may overlap other systemic diseases such as diabetes mellitus or hypertension. When ACS is clinically suspected in AI, biochemical tests are needed to establish the presence of cortisol excess. The screening tests include 24-hour urinary-free cortisol, 1 mg overnight dexamethasone suppression, and late-night salivary cortisol level, which refer to excessive cortisol secretion in a 24-hour period. These tests are the high sensitivity and specificity gold standard for diagnosis [2]. However, due to the long duration and cost, patients can leave the process halfway through without a diagnosis [1,10]. In conventional radiological evaluation, the separation of adenoma and non-adenoma is performed with high sensitivity and specificity with signal intensity measurement and calculations in MRI. However, it cannot be ascertained whether there is hormone secretion [11]. There is a need for cheaper and simpler tests of applicability in this area. The presented study shows that ACS could be well predicted using the radiomics score approach in AIs. In other words, the radiomics signature alone performed powerfully in classifying AIs.

Radiomics has developed rapidly in endocrine neoplasm practice in the past decade. In endocrine tumours

such as pituitary adenoma, thyroid nodules, and pancreatic neuroendocrine tumours, radiomics has been tested in many areas such as diagnosis, prognosis determination, and recurrence [12,13]. The application of radiomics in the adrenal gland is rarely reported [5,7].

Yu *et al.* evaluated the use of texture analysis for differentiation between benign and malignant adrenal lesions on contrast-enhanced abdominal CT. When analysing the texture, they only tested the parameters of the first order. They found that entropy and standard deviation demonstrated AUCs ranging from 0.91 to 0.97 for discriminating tumours, with sensitivities and specificities ranging from 73% to 95%, respectively [7]. In the presented study, a more complex texture analysis including first and second order was performed. Although the first order is a simpler texture analysis application, we think that more detailed information about texture can be obtained with second-order and high-order analyses.

Romeo *et al.* assessed the diagnostic efficacy of texture analysis extracted from MRI including T2W, T1W-Op, and T1W-Ip for characterizing AI (adrenal adenoma vs. non-adenoma). They obtained a diagnostic accuracy of 80% [14]. Similarly to Romeo *et al.*, the unenhanced MRI sequences (T1W and T2W) were used in the presented study. This is especially important for patients with impaired renal function due to the effects of hypercortisolism. Moreover, it provides an advantage in terms of cost. These sequences are traditional images, which can be achieved in a short time. The AUC of the radiomics score in T2W was increased to 0.994 compared to other phases of the study. However, to reach a definite conclusion, the most suitable sequences for texture analyses should be tested in future studies.

He *et al.* developed a clinical-radiomics on CT nomogram for the preoperative prediction of the APA risk in patients with unilateral adrenal adenoma. The nomogram showed good discrimination (AUC: 0.912) between NFA and APA [15]. In the presented study, the AUC of radiomics score to predict ACS was 0.994 (95% CI: 0.982-0.999), with a sensitivity of 0.94 and a specificity of 0.97. The clinical
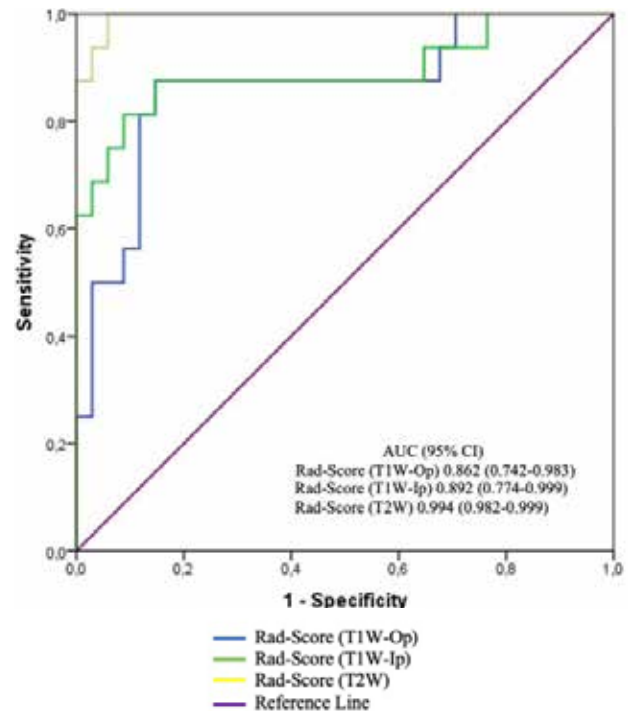


**Figure 2.** The receiving operating characteristics curves of the radiomics score on T1-weighted opposed-phase (T1W-Op), T1-weighted in-phase (T1W-Ip), and T2-weighted (T2W). ACS – adrenal Cushing syndrome, NFAI – non-functional adrenal incidentaloma

features did not use for the radiomics model, the use of additional clinical and laboratory parameters along with radiomic features may lead to better classification.

Zheng *et al.* explored the application value of multiparametric CT radiomics in differentiation between APA and cortisol-producing functional adrenocortical adenomas. ACSAI and ACS were placed in the same group [16]. A radiomics model yielded a sensitivity of 0.935, a specificity of 0.823, and an accuracy of 0.887 (AUC: 0.882, 95% CI: 0.819-0.945). They constructed a nomogram that achieved good discrimination performances, yielding a sensitivity of 0.915, a specificity of 0.928, and an accuracy of 0.922 (AUC = 0.902, 95% CI = 0.822-0.982). The nomogram included morphological radiologic fea-
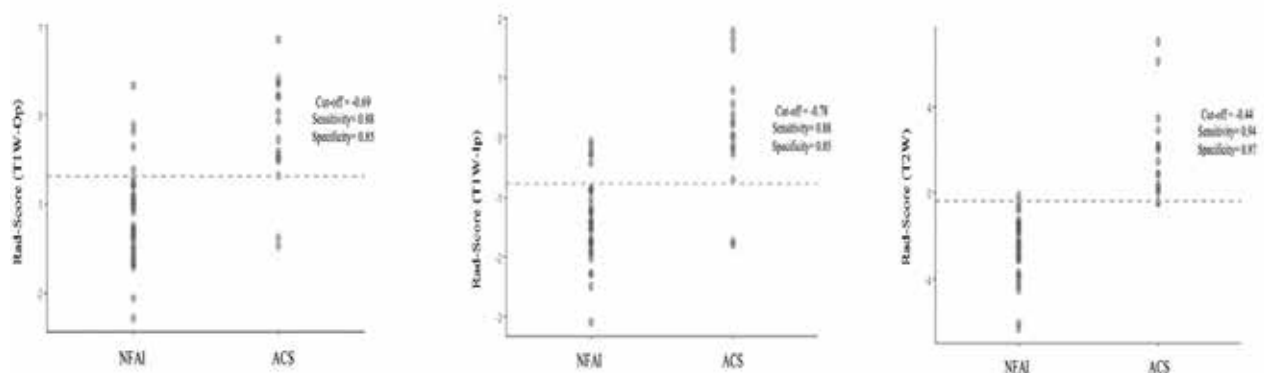


**Figure 3** A-C. Performance of radiomics score in discriminating adrenal Cushing syndrome (ACS) for 3 phases. Grey circles represent patients. The dashed lines indicate the cut-off value of the radiomics score. Patients above the threshold line were classified as ACS, while patients below the threshold line were classified as non-functional adrenal incidentaloma (NFAI). T1W – T1-weighted, Op – opposed-phase, Ip – in-phase, T2W – T2-weighted

tures such as contralateral adrenal size [16]. In the presented study, morphological radiologic features were not used, to reduce subjectivity.

The limitations of this study are the small sample size (especially the number of Cushing syndrome cases was limited) and the single-centre nature of the study. Therefore, validation by multicentre prospective studies is required prior to its wide use in clinical practice. Another limitation is that interobserver reproducibility in feature extraction could not be evaluated because only one radiologist was used to evaluate the images.

## Conclusions

The radiomics score reflects a perfect performance in differentiating between NFAI and ACS. The radiomics score has the potential to predict ACS with up to 94% accuracy. The developed MRI-based radiomic scores yielded high AUCs for the prediction of ACS for each phase.

## Conflict of interest

The authors report no conflict of interest.

## References

1. Araujo-Castro M, Sampedro Núñez MA, Marazuela M. Autonomous cortisol secretion in adrenal incidentalomas. Endocrine 2019; 64: 1-13.
2. Fassnacht M, Arlt W, Bancos I, et al. Management of adrenal incidentalomas: European Society of Endocrinology Clinical Practice Guideline in collaboration with the European Network for the Study of Adrenal Tumors. Eur J Endocrinol 2016; 175: G1-G34. doi: 10.1530/EJE-16-0467.
3. De Leo A, Mosconi C, Zavatta G, et al. Radiologically defined lipid-poor adrenal adenomas: histopathological characteristics. J Endocrinol Invest 2020; 43: 1197-1204.
4. Bancos I, Prete A. Approach to the patient with adrenal incidentaloma. J Clin Endocrinol Metab 2021; 106: 3331-3353.
5. Glazer DI, Mayo-Smith WW. Management of incidental adrenal masses: an update. Abdom Radiol 2020; 45: 892-900.
6. Stanzione A, Cuocolo R, Verde F, et al. Handcrafted MRI radiomics and machine learning: classification of indeterminate solid adrenal lesions. Magn Reson Imaging 2021; 79: 52-58.
7. Yu H, Parakh A, Blake M, et al. Texture analysis as a radiomic marker for differentiating benign from malignant adrenal tumors. J Comput Assist Tomogr 2020; 44: 766-771.
8. Unal I. Defining an optimal cut-point value in ROC analysis: an alternative approach. Comput Math Methods Med 2017: e3762651. doi: 10.1155/2017/3762651.
9. Hirsch D, Shimon I, Manisterski Y, et al. Cushing's syndrome: comparison between Cushing's disease and adrenal Cushing's. Endocrine 2018; 62: 712-720.
10. Pecori Giraldi F, Ambrogio AG. Variability in laboratory parameters used for management of Cushing's syndrome. Endocrine 2015; 50: 580-589.
11. Seo JM, Park BK, Park SY, et al. Characterization of lipid-poor adrenal adenoma: chemical-shift MRI and washout CT. Am J Roentgenol 2014; 202: 1043-1050.
12. Wang Y, Zhang L, Qi L, et al. Machine learning: applications and advanced progresses of radiomics in endocrine neoplasms. J Oncol 2021; 2021: 8615450. doi: 10.1155/2021/8615450.
13. Yi X, Guan X, Zhang Y, et al. Radiomics improves efficiency for differentiating subclinical pheochromocytoma from lipid-poor adenoma: a predictive, preventive and personalized medical approach in adrenal incidentalomas. EPMA J 2018; 9: 421-429.
14. Romeo V, Maurea S, Cuocolo R, et al. Characterization of adrenal lesions on unenhanced MRI using texture analysis: a machine-learning approach. J Magn Reson Imaging 2018; 48: 198-204.
15. He K, Zhang ZT, Wang ZH, et al. A clinical-radiomic nomogram based on unenhanced computed tomography for predicting the risk of aldosterone-producing adenoma. Front Oncol 2021; 11: 634879. doi: 10.3389/fonc.2021.634879.
16. Zheng Y, Liu X, Zhong Y, et al. A preliminary study for distinguish hormone-secreting functional adrenocortical adenoma subtypes using multiparametric CT radiomics-based machine learning model and nomogram. Front Oncol 2020; 10: 570502. doi: 10.3389/fonc.2020.570502.